

Phosphine adsorption and decomposition on Si(100) 2×1 studied by STM

Lutz Kipp,* R. D. Bringans, D. K. Biegelsen, J. E. Northrup, A. Garcia, and L.-E. Swartz
Xerox Palo Alto Research Center, 3333 Coyote Hill Road, Palo Alto, California 94304
(Received 28 October 1994; revised manuscript received 18 April 1995)

The adsorption and decomposition of phosphine molecules on clean Si(100) 2×1 surfaces have been investigated by scanning tunneling microscopy, photoemission spectroscopy, and total energy calculations. Phosphine decomposition depends strongly on the substrate temperature and results in a variety of surface structures depending on the relative rates of phosphine adsorption, hydrogen and phosphorus desorption, and hydrogen, phosphorus, and silicon surface diffusion. Between room temperature and 200 °C the phosphine mainly dissociatively adsorbs, most likely into P-P dimers. Near defect sites nondissociative adsorption of PH_3 is also found. For temperatures up to about 400 °C surface diffusion allows the generation of small P-P dimer rows. Above 400 °C, beyond the onset of hydrogen desorption, larger islands with width not exceeding approximately eight dimer rows are formed. At maximum phosphorus coverage, obtained by phosphine adsorption at 625 °C, straight vacancy lines are found, which most likely consist of phosphorus passivated Si(111) microfacets. Total energy calculations suggest that these may result from surface stress induced by the phosphorus overlayer.

I. INTRODUCTION

Heteroepitaxial growth of compound semiconductors such as GaAs and GaP on Si substrates is of significant technological importance since these systems may lead to many promising applications such as the monolithic integration of optical and electronic devices. Silicon substrates appear to be very reactive largely because of the presence of dangling bonds at the surface. In general, several monolayers can be added to these surfaces. Adsorption of As_4 , however, self-limits to one monolayer on Si(100) and has been found to fully coordinate and passivate this surface.¹ The chemical passivity of such monolayers is largely responsible for the three-dimensional growth of As-based III-V compounds on Si by molecular beam epitaxy (MBE).¹⁻⁴ For the heteroepitaxial growth of III As and III P compounds on silicon by metal-organic chemical vapor deposition the arsine and phosphine adsorption processes are of particular importance for an understanding of surface passivation and surfactant effects on the initiation of the heteroepitaxial growth process.

The adsorption and decomposition of arsine on Si(100) 2×1 has been discussed in detail in a previous paper.⁵ It was found that AsH_3 decomposes on the surface even at room temperature and four neighboring Si dangling bond sites are saturated in the process. At low coverages at room temperature, the main structure is most likely an arsenic monohydride bridge bonded to two Si dimers with two H atoms bound to the other end of the dimers. At higher temperatures and/or coverages, AsH_3 decomposition leads to As dimers and Si hydride. Depending on the relative rates of AsH_3 adsorption, H and As desorption, and H, As, and Si surface diffusion, a variety of island structures is formed.

The adsorption of PH_3 on Si(100) and its influence on

SiH_4 coadsorption was first studied by Yu and co-workers using low-energy electron diffraction, Auger electron spectroscopy, x-ray photoelectron spectroscopy (XPS), and thermal desorption spectroscopy.⁶⁻⁸ PH_3 was found to chemisorb on Si(100) and a strong temperature dependence of the phosphorus coverage at saturation showing a maximum for adsorption temperatures of about 550 °C was found.

PH_3 adsorption on Si(100) 2×1 at room temperature was studied by Wang *et al.* using scanning tunneling microscopy.⁹ They found evidence that the PH_3 molecule is adsorbed directly on top of a Si-Si dimer and proposed a nondissociative adsorption model in which the PH_3 molecule breaks the π bond of the Si-Si dimer and forms two Si-P bonds instead. In a very recent paper¹⁰ phosphine adsorption on Si(100) 2×1 at a substrate temperature of 550 °C was investigated. The scanning tunneling microscope (STM) images show a large number of long and narrow islands consisting primarily of P-P dimers on PH_3 saturated surfaces. These surfaces also contain large numbers of line defects perpendicular to the dimer rows, which were interpreted as acting as a stress relief mechanism. At lower P coverages obtained by either smaller PH_3 dosage at 550 °C or P desorption at 643 °C a significant number of Si-P dimers, but no line defects, were observed.¹⁰

Very recently Colaianni *et al.*¹¹ have reported on high-resolution electron energy loss spectroscopy (HREELS) and temperature programmed desorption (TPD) data of the adsorption and decomposition of PH_3 on Si(100) 2×1 surfaces in the temperature range 100–1000 K. For temperatures up to about 300 °C they observe Si-P, P-H, and PH_2 modes and up to about 400 °C Si-H bonds. The appearance of these modes confirms that the PH_3 has reacted with the silicon surface even at 100 K to produce adsorbed PH_n ($2 \geq n \geq 1$) and H species. TPD data

reveal PH_3 desorption peaks at 212 °C and 362 °C, the latter being due to recombinative desorption of PH_2 and hydrogen.

In this paper we present STM and XPS data for the adsorption and decomposition of PH_3 on $\text{Si}(100) 2 \times 1$ surfaces at substrate temperatures between room temperature (RT) and 750 °C and point out similarities as well as striking differences compared with AsH_3 adsorption on $\text{Si}(100)$. We also present first-principles total energy calculations for possible adsorption sites of PH_3 and calculations of the surface stress and energy for the P-terminated surface. In contrast to some of the interpretations in Refs. 9 and 10, we show in detail how a passivating phosphorus layer develops from PH_3 adsorption in the temperature range from room temperature to 625 °C. In particular, using STM in combination with XPS, we show that the maximum P coverage on $\text{Si}(100)$ is obtained for PH_3 adsorption at a substrate temperature of 625 °C, which is significantly higher than the rough estimate given by Yu and Meyerson (550 °C).⁶ Corresponding STM images show a full coverage of P-P dimers that are intersected by straight lines of missing dimers both perpendicular *and* parallel to the dimer rows. It will be shown further that the formation of Si-P heterodimers depends on substrate temperature rather than P coverage as proposed recently.¹⁰

After describing the experimental details, we will discuss the PH_3 adsorption results in different temperature regimes. We begin with adsorption at room temperature, then discuss the effects of surface diffusion and hydrogen desorption at intermediate temperatures and how they are related to P coverages and surface structures.

II. EXPERIMENTAL DETAILS

The experiments were carried out in an ultrahigh vacuum (UHV) system consisting of different isolatable chambers disposed radially about a central sample exchange manipulator. The chambers are (i) a well characterized MBE system, which contains an As_4/As_2 solid evaporation source and AsH_3 and PH_3 gas inlets; (ii) a chamber for angle resolved photoemission, Auger spectroscopy, and low-energy electron diffraction (LEED) studies; (iii) an XPS system using Al $K\alpha$ radiation (VG ESCALAB MK1), and (iv) a scanning tunneling microscope as described elsewhere.¹²

The $\text{Si}(100)$ samples were cut from polished wafers [P-doped (*n*-type), 0.01 Ω cm, on axis to ± 0.25 °C] and pre-cleaned *ex situ* by submerging in a 1:1 solution of H_2SO_4 and H_2O_2 for 10 min. After rinsing in deionized water they were dipped in HF for 30 sec, rinsed again, and then finally oxidized in an ozone environment for about 2 min. After insertion into the UHV system the samples were outgassed at 600 °C for several hours using Ohmic direct heating. A final quick annealing to 1200 °C for 30 sec always led to clean $\text{Si}(100) 2 \times 1$ reconstructed surfaces as characterized by LEED, XPS, and STM. The substrate temperature was measured with an optical pyrometer (IRCON 300 C).

Phosphine exposures were performed using a leak valve in the MBE system. The relative coverage of phospho-

rus on silicon was determined from the area ratios of the P 2*p* and Si 2*p* peaks in the XPS spectra. Since a reference monolayer (ML) of phosphorus is not as easily obtained as an As monolayer on $\text{Si}(100)$, absolute P coverages are difficult to obtain from the XPS data alone. A first estimate of the coverage was obtained by using an As monolayer as a standard and then using the relative photoemission cross sections calculated¹³ for P 2*p* and As 3*d*. This leads to an area ratio (P 2*p*/Si 2*p*) $\sim 0.64 \times$ (As 3*d*/Si 2*p*) for equivalent submonolayer coverages. A reference monolayer of As is known to be achieved by exposing clean $\text{Si}(100) 2 \times 1$ to 1×10^{-6} Torr As_4 from a solid As source at 700 °C sample temperature followed by 1 min of annealing to 300 °C at base pressure.¹ Evaluation of the STM images in combination with XPS results, however, gives more accurate information on P coverages as shown below. Although PH_3 is extremely sensitive to decomposition by electron beams, we tested for and did not observe any decomposition induced by, e.g., ion gauges in the system. STM images were taken at room temperature with a constant tunneling current of 50 pA. Positive tip bias voltages correspond to electrons tunneling out of the occupied surface states of the sample.

III. RESULTS AND DISCUSSION

Normalized XPS results for saturated phosphorus coverages obtained from 50 Langmuir (L) ($1 \text{ L} \equiv 10^{-6}$ Torr sec) PH_3 fluence ($p = 5 \times 10^{-7}$ Torr) on $\text{Si}(100) 2 \times 1$ at different substrate temperatures are shown in Fig. 1. Several different temperature regimes are observed: For substrate temperatures up to about 150 °C, P saturation coverages of about 1/5 of the maximum coverage are obtained. In the temperature regime between $\sim 150^\circ$ and 400 °C, slightly lower P coverages ($\sim 1/6$) are found. The higher coverage for RT adsorption may be correlated with additional PH_n ($n=0, \dots, 3$) species physisorbed on top of the first layer which can be easily desorbed at temperatures above ~ 150 °C. At elevated temperatures (above ~ 400 °C) the hydrogen desorbs [this was also found for AsH_3 adsorption on $\text{Si}(100)$

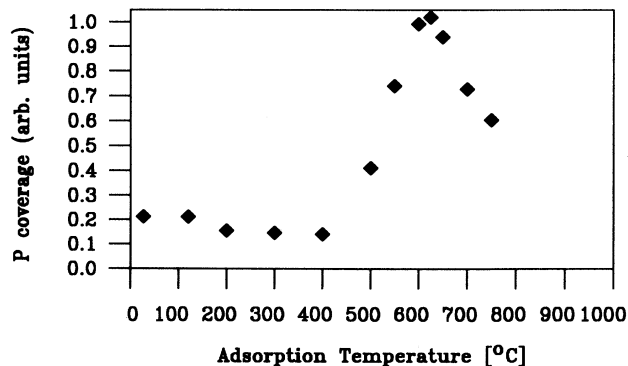


FIG. 1. Phosphorus coverage obtained for 50 L of PH_3 exposure of $\text{Si}(100) 2 \times 1$ at substrate temperatures from RT to 750 °C followed by 2 min of annealing at 300 °C (for exposures ≥ 300 °C).

2×1], thereby freeing up more space for the incoming PH_3 molecules. Thus the P coverage increases and it reaches a maximum around 625°C . For temperatures above 625°C , the P itself starts to desorb. These results are very similar to those obtained for AsH_3 adsorption⁵ on $\text{Si}(100) 2 \times 1$. Using the calculated photoemission cross sections for the determination of absolute P coverages would result in 0.9 ML for the maximum value in Fig. 1. The uncertainty in the cross sections and the different kinetic energies and angular momenta of As $3d$ and P $2p$ photoelectrons, however, may lead to a large systematic error. We argue below, based on STM images, that the peak coverage is in fact slightly greater than 1.0. (We note that a qualitatively similar behavior of low and high coverage regimes has also been seen by Yu and Meyerson⁶ using Auger electron spectroscopy. As noted above, the maximum P coverage they observed, however, occurred after PH_3 adsorption at 550°C .)

A. Phosphine uptake at low temperature

Figure 2 shows an image of $\text{Si}(100)$ after RT exposure to 0.05 L of PH_3 (far below the saturation fluence). The image reveals a random distribution of light gray and white spots located on top of the Si dimer rows of the substrate. Single height atomic steps of the Si substrate can also be seen. Most features are oblong in shape and centered on the Si dimer rows (see inset), suggesting that a P-P dimer deriving from two PH_3 molecules is inserted across (orthogonal to) two Si dimers. Minimization of the number of dangling bonds on the surface will occur if all hydrogen atoms transfer to Si dangling bonds, resulting in one P-P dimer. This is in contrast to the off-center position seen for AsH_3 adsorption on $\text{Si}(100)$ at RT,⁵ which

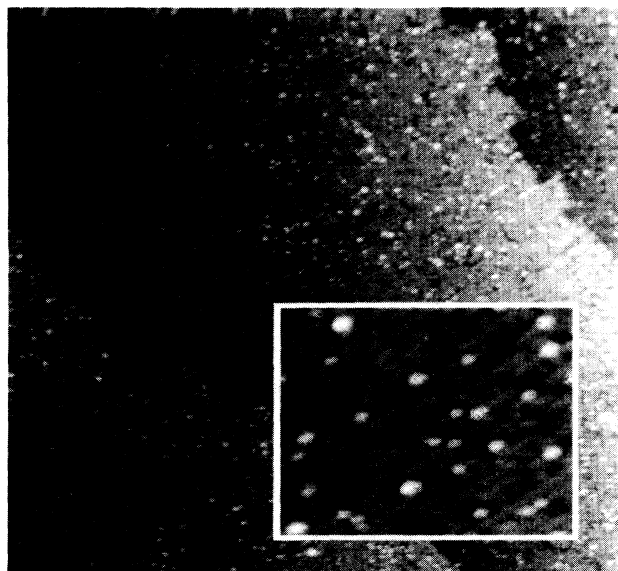


FIG. 2. STM filled states images (+2 V bias) of $\text{Si}(100)$ after exposure to 0.05 L of PH_3 at room temperature. The horizontal dimension of the lower-magnification image is ~ 90 nm.

was attributed to a single As-H unit where one As atom is bridge bonded to two silicon atoms on adjacent dimers. The same dangling bond minimization can occur with one P-P dimer, two Si-P dimers, or a Si-Si dimer plus two P atoms in substitutional bulk sites. Therefore, we cannot rule out the possibility that the dimers observed are Si-P or Si-Si. At these low adsorption temperatures, however, it is likely that kinetic barriers prevent significant Si-P exchange from taking place.

The fact that P-P dimers form at very low coverage suggests that PH_n molecules are mobile on the surface, even at RT, until they form dimers or are eventually trapped at defects (see larger white features in the inset). Evidently no ordering occurs at this temperature, indicating a lack of surface dimer diffusion.

On the basis of thermal desorption spectroscopy Yu and Meyerson⁶ proposed that PH_3 molecules would adsorb nondissociatively and suggested that a PH_3 molecule could bind directly above a Si-Si dimer, resulting in fivefold coordinated P atoms. More recently, Wang *et al.*⁹ interpreted their STM data to show the existence of such a pentacoordinate structure. However, we cannot confirm these results on the basis of our STM data as well as the HREELS spectra of Colaianni *et al.*¹¹ Bonding of PH_n at defect sites is, however, energetically more favorable and the STM image in Fig. 2 shows some features that may correspond to this situation.

To test the stability of the PH_3 adsorption site proposed by Yu and Meyerson,⁶ we performed total energy calculations. As in previous calculations for AsH_3 on $\text{Si}(100)$ ¹⁴ the momentum space pseudopotential formalism¹⁵⁻¹⁷ and the local density approximation were employed. Atomic positions were determined by calculations of the Hellmann-Feynman forces. The kinetic energy cutoff for the wave functions was taken to be 10 Ry and Brillouin zone averages were performed with four k points. A 2×2 unit cell with two Si-Si dimers and one PH_3 molecule located above one of the dimers was employed.

The calculations for a PH_3 molecule located above the center of a Si-Si dimer show that the molecule interacts with the surface only very weakly in this configuration, with Si-P distances in the range of 2.6–2.7 Å. The calculated total energy is only -0.25 eV relative to the bare $\text{Si}(100)$ surface and a free molecule. In addition, this structure is found to be unstable with respect to binding of the PH_3 directly to one of the Si dangling bonds of the Si-Si dimer. In this configuration the P atom is fourfold coordinated with a Si-P bond length of 2.37 Å and the binding energy is -1.08 eV. The energy difference between the fivefold and the fourfold configurations is 0.83 eV. This is much larger than the calculational uncertainty, which is less than 0.1 eV. Although the possibility of a nondissociated fourfold PH_3 is not excluded by these calculations, the results of Colaianni *et al.*¹¹, which indicate that dissociation occurs even at 100 K, suggest that there is no barrier for the fourfold PH_3 to shed a hydrogen atom and become Si- PH_2 and Si-H. On the basis of these results it seems unlikely, therefore, that PH_3 exists in the proposed fivefold coordinated configuration.

A full coverage with *isolated* P-P dimers and surround-

ing Si-H would result in 20–33% P coverage (20% if we assume that H atoms do not bond to the same Si atoms that are bonded to the P-P dimer and 33% if we assume that H atoms can bond to any available dangling bond). Physisorbed PH_n can increase the coverage at RT but should be easily removed at slightly higher temperatures. This is likely seen in Fig. 1, where the P coverage decreases for substrate temperatures in the range 200 °C–400 °C. Thermal desorption spectra for PH_3 on Si(100) show a peak at 275 °C from a room temperature adsorbed PH_3 layer on Si(100).⁸ It is not evident, however, whether this desorption peak reveals mainly the desorption of physisorbed PH_3 , PH_3 bonded to defect sites, or PH_3 adsorbed in a pentavalent configuration on top of a Si-Si dimer. The estimated activation energy of 0.6 eV (Ref. 8) could explain reasonably well the PH_3 desorption from defect sites. TPD results¹¹ employing isotopic exchange studies were interpreted to show that PH_3 desorption at 362 °C is due to a recombination of PH_2 and surface hydrogen. Stable tunneling conditions at saturation coverage for RT PH_3 adsorption could not be achieved. This may be due to physisorbed or very weakly chemisorbed PH_n species that can be easily picked up with the tunneling tip. The higher P coverage at RT saturation is most likely due to these species. The $c(4 \times 2)$ ordering after RT adsorption of PH_3 seen by Wang *et al.*⁹ and attributed to ordered arrangements of PH_3 molecules, which would give 25% P coverage for perfect ordering, is not reproduced in our experiments. However, the vibrational spectroscopy results of Colaianni *et al.*¹¹ clearly show that PH_3 is dissociatively adsorbed even at 100 K.

If the adsorption temperature is increased to 350 °C significant diffusion and ordering take place. We find that most of the single P-P dimers that were present after adsorption at RT have coalesced to form short rows perpendicular to the underlying dimer rows. This is shown in Fig. 3 for a Si(100) 2×1 surface following exposure to 0.05 L of PH_3 at 350 °C.

Shown in Fig. 4 is a STM image of the Si(100) 2×1 surface following exposure to 50 L of phosphine at 350 °C. XPS measurements made as a function of exposure showed that the surface is fully saturated with phosphine. We can see rows of dimers lying above the underlying dimer rows and oriented perpendicular to them. These upper rows occasionally appear side by side, but for the most part they are isolated from one another. Crossing the image are one-atom-high steps. This surface is very similar to the one obtained by AsH_3 saturation at 410 °C (cf. Ref. 5). The underlying rows of Si dimers evident in Fig. 4 are presumably passivated with hydrogen since no further adsorption occurs. Evidently no or only very few P atoms are incorporated in the second layer. This can be seen by the absence of speckles, in the underlying dimer rows. Such speckles, which are due to the different density of states in the available energy range around P and Si atoms, are observed for a mixed P-Si layer (see below).

B. Adsorption at RT plus subsequent annealing

A STM image obtained after 0.5 L of PH_3 exposure at RT and subsequent 5 min of annealing at 350 °C is

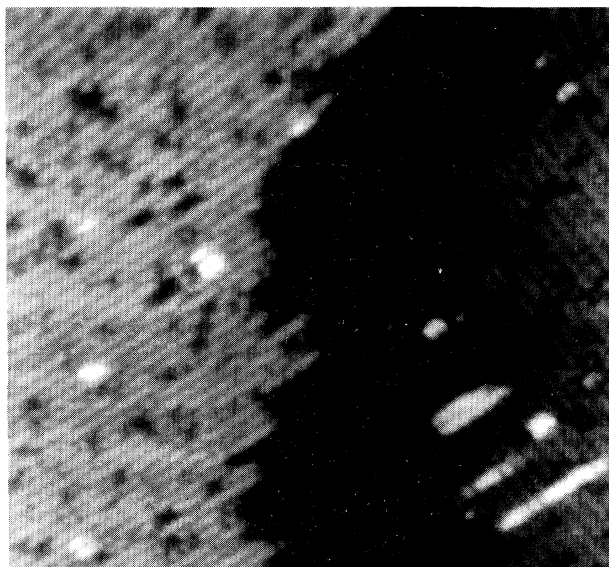


FIG. 3. STM filled state image (+2 V bias) of 0.05 L of PH_3 adsorption on Si(100) 2×1 at 350 °C substrate temperature. The horizontal dimension is ~ 33 nm.

presented in Fig. 5. In this case one can see a number of relatively short (approximately three to six dimers long) P-P dimer rows perpendicular to the underlying Si dimer rows. Very few isolated dimers can be observed. This surface is very similar to that shown in Fig. 4. Larger islands containing more than three P-P dimer rows in parallel are not found at 350 °C. At this temperature, which is below the onset of H desorption, approximately three times as much hydrogen as phosphorus must be present on the

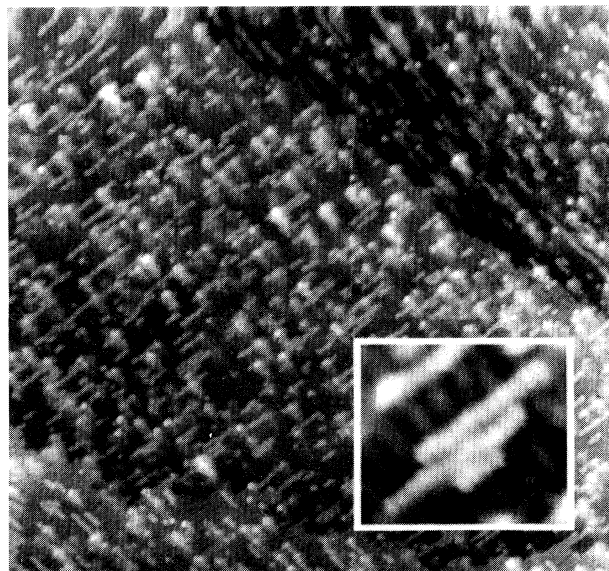


FIG. 4. STM filled state images (+2 V bias) of 50 L of PH_3 adsorption on Si(100) 2×1 at 350 °C substrate temperature. The horizontal dimension of the lower-magnification image is ~ 90 nm.

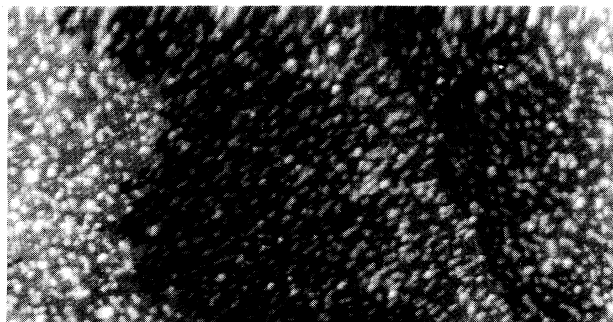


FIG. 5. STM filled state image (+2 V bias) following 0.5 L of PH_3 exposure at RT and annealing the substrate 5 min at 350°C . The horizontal image size is about 90 nm.

surface. It is most likely the hydrogen that hinders the dimer diffusion and the formation of larger islands. This is further corroborated by the image in Fig. 6 obtained after 5 L of PH_3 dosage at RT followed by a 5 min of annealing at 450°C . This annealing temperature is beyond the onset of H desorption (cf. Fig. 1) and larger islands can now be formed. The randomly adsorbed P dimers have coalesced into islands of dimers containing up to about eight dimer rows. It appears that the islands may contain Si in either Si-Si or Si-P dimers since some of the dimers in these structures are observed to be buckled. The islands cover $\sim 20\%$ of the surface. Given the 20% P coverage we expect for saturation with P-P dimers and Si-H and that no phosphorus is desorbed at this temperature (see Fig. 1) we conclude that these islands reveal the predominant coalescence of phosphorus in Si-P and P-P dimers in the first two atomic layers.

We find that we only see the dimer rows and dimer islands when P is present on the surface. Annealing a

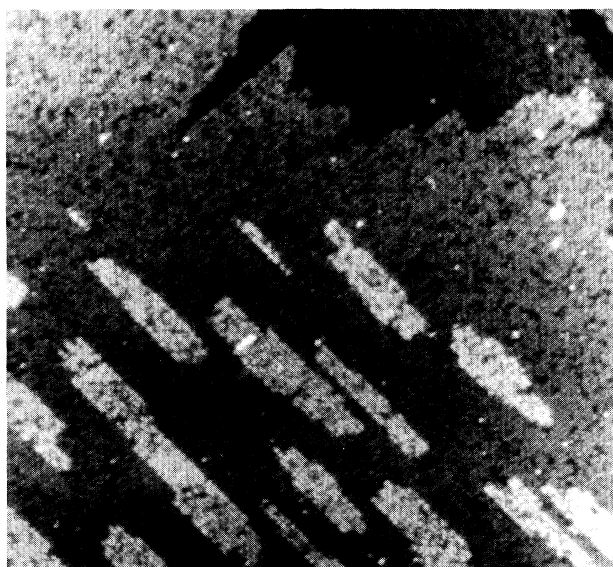


FIG. 6. STM filled state image (+2 V bias) following 5 L of PH_3 exposure at RT and annealing the substrate 5 min at 450°C . The horizontal image size is about 90 nm.

surface after RT adsorption of 50 L of PH_3 (saturation) for 150 sec at 680°C results in a clean surface showing no islands. The coverage with phosphorus in this case is below our detection limit. The formation of islands at 450°C annealing was also observed for AsH_3 on Si(100) reflecting the close similarity of both systems at these temperatures.

C. Phosphine uptake at 625°C

At temperatures around 625°C , we reach a regime yielding complete hydrogen desorption. The P coverage can be increased to its maximum value as shown in Fig. 1. A STM image obtained after dosing clean Si(100) 2×1 with 50 L of PH_3 at 625°C , cooling down below 200°C in a PH_3 flux ($p = 5 \times 10^{-7}$ Torr), and subsequent 2 min of annealing at 300°C is presented in Fig. 7. The image shows P-P dimer rows containing only symmetric dimers. The larger features on top suggest the presence of PH_n species. In addition, we observe a number of straight rows of missing dimers either perpendicular or parallel to the phosphorus dimer rows. This contrasts significantly with the results for 1 ML of As on Si(100), where a perfect layer of As dimer rows is seen.¹⁸

Figure 8 shows a large scale image ($\sim 90 \times 90 \text{ nm}^2$) of the surface presented in Fig. 7 after an additional 5 min of annealing at 500°C . We observe that the superficial species are desorbed at this temperature and obtain a more detailed insight into the distribution of the straight lines of missing dimers. Basically two different types of these lines are observed. Close to step edges we find a strong driving force for generating missing dimer rows parallel to the P dimer rows. These missing rows are

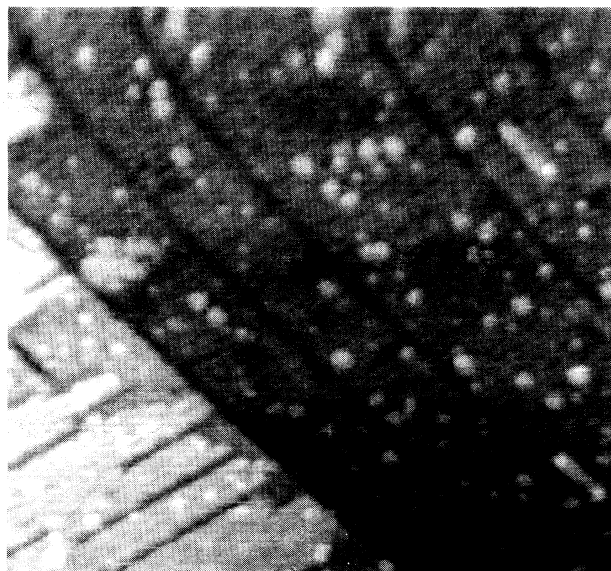


FIG. 7. STM filled state image (+2 V bias) of 50 L of PH_3 adsorption at 625°C substrate temperature with subsequent 2 min of annealing at 300°C . The horizontal dimension is $\sim 33 \text{ nm}$.

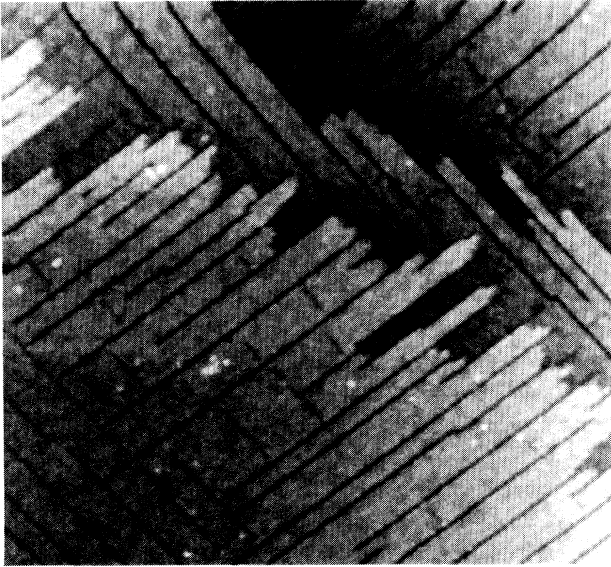


FIG. 8. Large scale ($\sim 90 \times 90 \text{ nm}^2$) STM filled state image (+2 V bias) of the surface shown in Fig. 7 after an additional 5 min of annealing at 500°C . The horizontal dimension is $\sim 90 \text{ nm}$.

separated by approximately four to eight dimer rows. Towards the middle of larger terraces the direction of vacancy lines is rotated by 90° now appearing perpendicular to the P dimer rows. The two types of vacancy lines generally do not intersect. Most of the vacancy lines end a few dimers before they touch a line of the other type. A similar behavior is found close to step edges where the vacancy lines also end a few dimer lengths before the edge. This behavior is consistent with stress being the driving force for the generation of vacancy lines. Ordered vacancy lines *perpendicular* to dimer rows are also seen¹⁹ for 1.5 ML of Ge on Si(100) and P on Si(100) below the saturation coverage,¹⁰ but not for As on Si(100). The atomic structure of the vacancy lines observed here, however, cannot simply be explained by missing P-P dimers alone. As is evident from the STM image shown in Fig. 11, some of the rows of missing dimers parallel to the dimer rows continue over monoatomic steps to form vacancy lines perpendicular to the dimer rows. This is shown schematically in Fig. 9. A possible atomic structure is shown in Fig. 10. The vacancy lines parallel to the dimer rows (left) are generated by removing a top layer dimer row and second to fourth layer Si atoms. The top Si atoms of the Si(111) facets are most likely exchanged by phosphorus atoms to reduce the number of dangling bonds. Vacancy lines perpendicular to the dimer rows (right) reach down to the same layer and two dimers in parallel have to be removed in the top layer. For each removed P atom in the vacancy lines of either type two additional P atoms can be incorporated in the (111) facets.

It is likely that stress relief is the driving force for the formation of the trenches observed on the Si(100) P-terminated surface. Specifically we propose that the formation of P-terminated (111) microfacets allows the tensile stress parallel to the P-P dimer to be relieved.

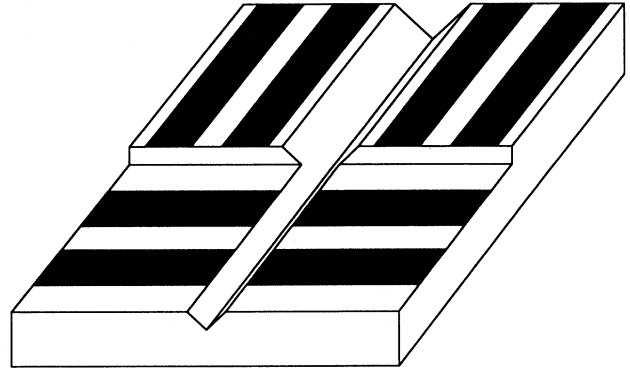


FIG. 9. Schematic of a vacancy line parallel to P-P dimer rows (black bars) that continues over monoatomic steps and appears then as vacancy line perpendicular to the dimer rows.

In calculations of the surface stress tensor for the Si(100) 2×1 P surface, performed as discussed in Ref. 20, we find a tensile stress of $3.0 \text{ eV}/(1 \times 1)$ in the direction parallel to the P-P dimer and a stress of $3.5 \text{ eV}/(1 \times 1)$ in the direction perpendicular to the dimer. These stresses are much larger than those found on the bare Si(100) surface and result from the tendency of P (like As) to prefer p^3 hybridization.^{20–22} It is therefore plausible that the (111) facets relieve the stress by allowing the (100) terraces to relax along the dimer direction. However, for stress relief to be effective in reducing the energy, the formation energy of the facets must not be prohibitive. The energy cost of the (111) facet should be sufficiently low so that stress relief results in an overall reduction in energy. On the other hand, if the formation of (111) facets were strongly exothermic, then one would expect to see macroscopic faceting. Since the proposed microfacets consist of P-terminated Si(111) 1×1 we calculated the surface energy of the Si(111) 1×1 P-terminated surface. From this energy and the surface energy of the Si(100) 2×1 P surface we may obtain an estimate of the formation energy of a (111) microfacet on the P-terminated Si(100) surface.

The surface energy for the P-terminated Si(100) 2×1 and P-terminated Si(111) 1×1 surfaces depend on the chemical potential μ_P of the phosphorus. For the Si(100) 2×1 P surface we obtain a surface energy

$$E_{100}(\text{eV}/1 \times 1) = 0.37 + \Delta\mu, \quad (1)$$

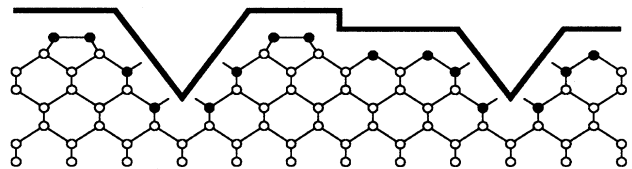


FIG. 10. Possible atomic structure of vacancy lines parallel (left) and perpendicular (right) to dimer rows on phosphorus passivated Si(100). The trenches are generated by Si(111):P microfacets to relieve stress and reduce the number of dangling bonds. P and Si atoms are plotted as full and open circles.

where $\Delta\mu$ denotes the chemical potential of P measured with respect to its value in bulk P

$$\Delta\mu = \mu_{\text{P(bulk)}} - \mu_{\text{P}}. \quad (2)$$

Because precipitation of bulk P will prevent μ_{P} from exceeding $\mu_{\text{P(bulk)}}$, $\Delta\mu$ is always positive under equilibrium conditions. The surface energy for bare Si(100) is approximately $1.39 \text{ eV}/(1 \times 1)$;²³ thus for Si(100) 2×1 P to be stable with respect to the bare surface we must have $\Delta\mu < 1 \text{ eV}$. For Si(111) 1×1 P the calculated surface energy is

$$E_{111}(\text{eV}/1 \times 1) = 0.14 + \Delta\mu. \quad (3)$$

From these results we may estimate the formation energy of a 111 facet. To create a facet we replace a 2×1 unit cell of Si(100) P with four 1×1 unit cells of the P-terminated (111) surface. Therefore an estimate for the formation energy of a microfacet is

$$\Omega_{111\text{facet}} = 4E_{111} - 2E_{100} = -0.18 + 2\Delta\mu \quad (4)$$

in units of eV/a , where $a = 3.83 \text{ \AA}$ is the lattice constant along the dimer row direction. The formation energy is very low and in fact becomes negative when μ_{P} approaches $\mu_{\text{P(bulk)}}$. In this approximation, for sufficiently high P chemical potentials ($\Delta\mu < 0.09 \text{ eV}$) the faceted surface will become more stable than the Si(100) 2×1 P surface. For comparison, if the (111) microfacet were not terminated by P, and since the surface energy of the bare Si(111) surface is roughly $1.2 \text{ eV}/(1 \times 1)$,²² the formation energy of the facet would be very high; $\Omega_{(111)\text{facet}} = 4.0 - 2\Delta\mu$. From this it is clear that facet formation requires the presence of P to passivate the exposed (111) microfacets and that facet formation becomes possible for reasonable values of the P chemical potential. On the other hand, because the facets are seen to have very nearly a constant width, the chemical potential of P is evidently not sufficiently high to drive macroscopic (111) faceting.

This approximation for Ω_{facet} does not include the relaxation energy, which results from the stress reduction enabled by the microfacets. Stress relief will further stabilize microfacets on the Si(100) P surface. Our picture, then, is that the presence of P lowers the surface energy for both (100) and (111) faces and thereby enables surface corrugation to occur without increasing the total energy and the corrugation allows surface stress to be relieved. The relatively constant spacing between trenches seems to confirm the notion that the facets are nucleated to relieve terrace stress.

The average areal density of vacancy lines both parallel and perpendicular to dimer rows was measured over a number of images and found to be $\sim 25\%$. The remaining $\sim 3/4$ of the surface is covered with P-P dimers. Because we can place twice as many P atoms in the trenches as compared to the flat surface, the resulting phosphorus coverage would be about 125% in this case. Scaling the maximum coverage in Fig. 1 to 125% would result in 25% coverage for saturation at RT and 20% between $\sim 200^\circ$ and 400° C . This is in reasonable agreement with the 20% saturation coverage obtained with P-P dimers and Si-H

(plus some RT physisorbed PH_n molecules, that can easily be desorbed). It also supports the conclusion that the formation of islands covering $\sim 20\%$ of the surface (see Fig. 6) is directly related to the phosphorus coverage. It is important to note that the absolute calibration of P coverages using relative coverages obtained by XPS in combination with STM results gives a consistent picture of the data described here. Using XPS data alone plus calculated cross sections and normalization to an As monolayer results in P coverages that are smaller ($\sim 90\%$ coverage for the maximum value), but the uncertainty in this approach is of the order of 50%.

Details of the structure of this surface are revealed in filled and empty states STM images taken at larger magnification. In Fig. 10 we show STM images of the same region tunneling out of (left panel) and into (right panel) the surface. In addition to the vacancy lines we now observe intensity variations within the dimer rows. The dimers appear white, gray, or white on one side and gray on the other. This suggests that the dimer rows contain, in addition to P-P dimers, Si atoms either in Si-Si or Si-P dimers. The STM image taken before the 500° C anneal in contrast shows only dimers of one type (see Fig. 7). The P coverage as obtained by XPS has not decreased significantly (less than $\sim 10\%$; see Fig. 12). This may be due to desorption of a physisorbed species or a small reduction in the detected photoemission intensity due to Si-P exchange in the outermost layers. Furthermore, we observe a ratio of approximately 50:50 for white to gray features. We therefore conclude that some phosphorus atoms must have switched into the second layer. Diffusion of phosphorus atoms far into the bulk Si can be ruled out because of the surface sensitivity of photoemission.

We note that we observed the development of a passivating P layer on Si(100) starting with P-P dimers at

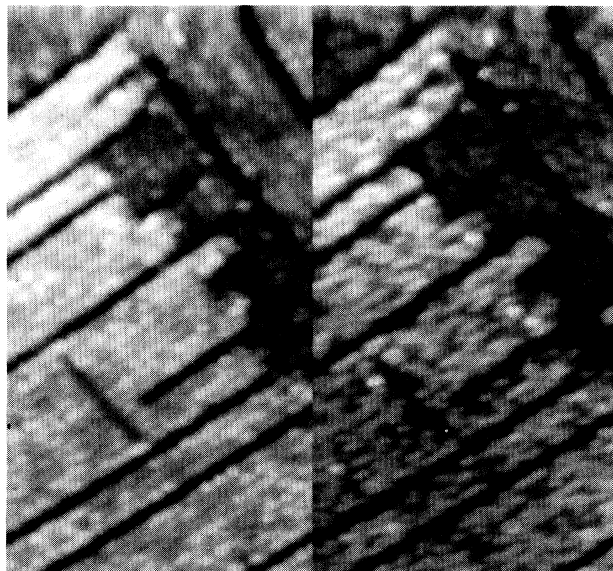


FIG. 11. STM images [$+1.8 \text{ V}$ (left) and -1.8 V bias (right)] of the surface shown in Fig. 7 after an additional 5 min of annealing at 500° C . The horizontal dimension is about 33 nm.

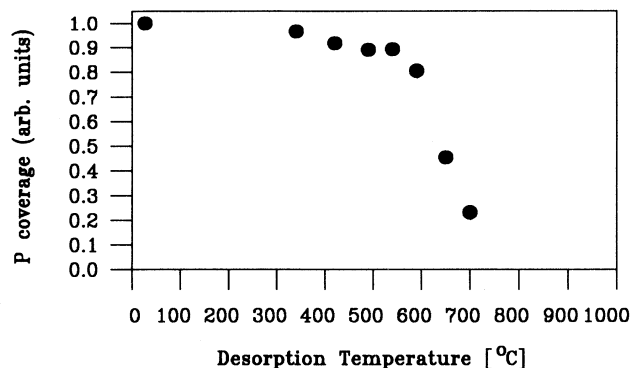


FIG. 12. Phosphorus desorption in UHV from a surface prepared by a 50 L of PH_3 dosage of Si(100) 2×1 at 625°C . Each point represents a 2-min annealing step at that temperature.

RT and the formation of P-P dimer strings for PH_3 saturation at temperatures below the onset of H desorption for PH_3 exposure at $p = 5 \times 10^{-7}$ Torr. There was no evidence of the formation of large numbers of Si-P heterodimers under these experimental conditions. Prolonged annealing at temperatures above $\sim 450^\circ\text{C}$, however, results in a mixture of Si-Si, Si-P, and P-P dimers contained in the top (two) layers (see Figs. 6 and 11).

IV. CONCLUSIONS

We have studied the adsorption and decomposition of phosphine on Si(100) for temperatures between room temperature and 750°C using STM, XPS, and total energy calculations. It was found that most PH_3 molecules decompose on the surface even at room temperature and the main structure is most likely a phosphorus dimer sitting on top of the Si dimer rows. At higher temperatures and/or coverages, PH_3 decomposition leads to short chains of P dimers and Si hydride. At full coverage with phosphorus, stress acts as a driving force for the generation of straight lines of dimer vacancies parallel and perpendicular to dimer rows. These vacancy lines most likely consist of P passivated Si(111) microfacets. Interfacial mixing and the formation of island structures containing a mixture of Si-Si, P-P, and Si-P dimers is observed after annealing at temperatures above $\sim 450^\circ\text{C}$.

ACKNOWLEDGMENTS

We are pleased to acknowledge discussions of this work with Jörg Neugebauer. A. G. and J. E. N. were supported in part by the ONR Contract No. N00014-92-C0009.

* Permanent address: Institut für Experimentalphysik, Universität Kiel, Olshausenstraße 40, 24098 Kiel, Germany.

¹ R. D. Bringans, *CRC Crit. Rev. Solid State Mater. Sci.* **17**, 353 (1992).

² J. E. Northrup, *Phys. Rev. Lett.* **62**, 2487 (1989).

³ D. K. Biegelsen, L.-E. Swartz, and R. D. Bringans, *J. Vac. Sci. Technol. A* **8**, 280 (1990).

⁴ E. Kaxiras and J. D. Joannopoulos, *Surf. Sci.* **224**, 515 (1989).

⁵ L. Kipp, R. D. Bringans, D. K. Biegelsen, L.-E. Swartz, and R. F. Hicks, *Phys. Rev. B* **50**, 5448 (1994).

⁶ M. L. Yu and B. S. Meyerson, *J. Vac. Sci. Technol. A* **2**, 446 (1984).

⁷ B. S. Meyerson and M. L. Yu, *J. Electrochem. Soc.* **131**, 2366 (1984).

⁸ M. L. Yu, D. J. Vitkavage, and B. S. Meyerson, *J. Appl. Phys.* **59**, 4032 (1986).

⁹ Y. Wang, M. J. Bronikowski, and R. J. Hamers, *J. Phys. Chem.* **98**, 5966 (1994).

¹⁰ Y. Wang, X. Chen, and R. J. Hamers, *Phys. Rev. B* **50**, 4534 (1994).

¹¹ M. L. Colaianni, P. J. Chen, and J. T. Yates, *J. Vac. Sci. Technol. A* **12**, 2995 (1994).

¹² D. K. Biegelsen, R. D. Bringans, J. E. Northrup, and L.-E. Swartz, *Phys. Rev. B* **41**, 5701 (1990).

¹³ J. J. Yeh and I. Lindau, *At. Data Nucl. Data Tables* **32**, 1 (1985).

¹⁴ J. E. Northrup, *Phys. Rev. B* **51**, 2218 (1995).

¹⁵ J. Ihm, A. Zunger, and M. L. Cohen, *J. Phys. C* **12**, 4409 (1979).

¹⁶ M. T. Yin and M. L. Cohen, *Phys. Rev. B* **26**, 5668 (1982).

¹⁷ G. B. Bachelet and M. Schlüter, *Phys. Rev. B* **25**, 2103 (1982).

¹⁸ R. D. Bringans, D. K. Biegelsen, and L.-E. Swartz, *Phys. Rev. B* **44**, 3054 (1991).

¹⁹ X. Chen, F. Wu, Z. Zhang, and M. G. Lagally, *Phys. Rev. Lett.* **73**, 850 (1994).

²⁰ A. Garcia and J. E. Northrup, *Phys. Rev. B* **48**, 17350 (1993).

²¹ R. D. Meade and D. Vanderbilt, in *Proceedings of the Twentieth International Conference on the Physics of Semiconductors*, edited by E. M. Anastassakis and J. D. Joannopoulos (World Scientific, Singapore, 1990).

²² R. D. Meade and D. Vanderbilt, *Phys. Rev. Lett.* **63**, 1404 (1989).

²³ J. E. Northrup, *Phys. Rev. B* **47**, 10032 (1993).

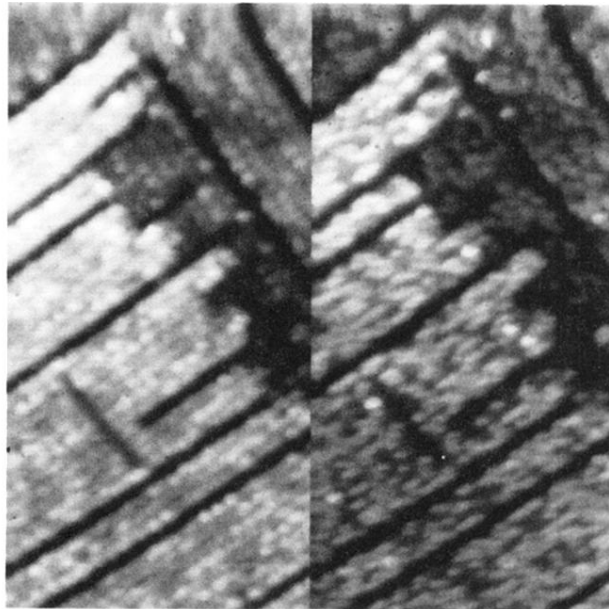


FIG. 11. STM images [$+1.8$ V (left) and -1.8 V bias (right)] of the surface shown in Fig. 7 after an additional 5 min of annealing at 500°C . The horizontal dimension is about 33 nm.

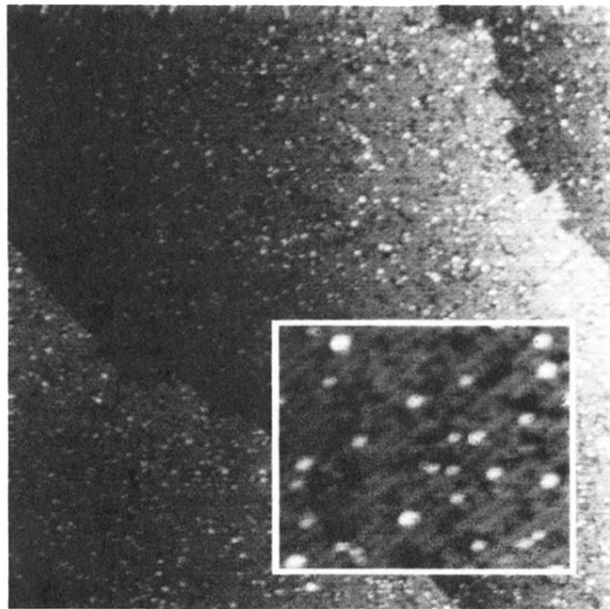


FIG. 2. STM filled states images (+2 V bias) of Si(100) after exposure to 0.05 L of PH_3 at room temperature. The horizontal dimension of the lower-magnification image is ~ 90 nm.

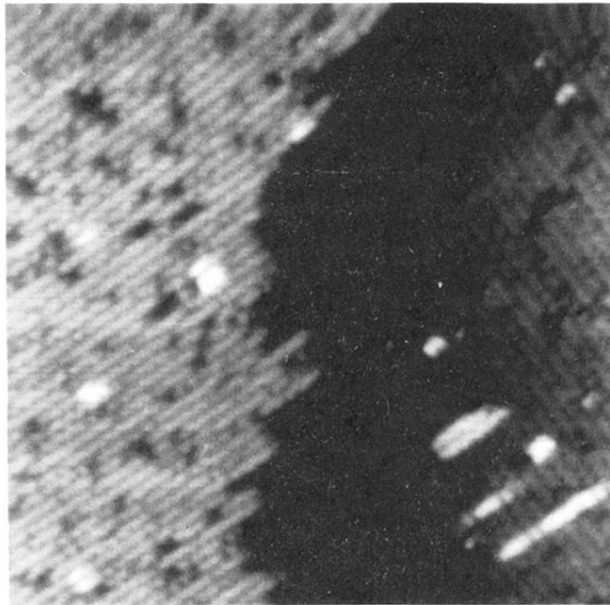


FIG. 3. STM filled state image (+2 V bias) of 0.05 L of PH_3 adsorption on $\text{Si}(100) 2 \times 1$ at 350°C substrate temperature. The horizontal dimension is ~ 33 nm.

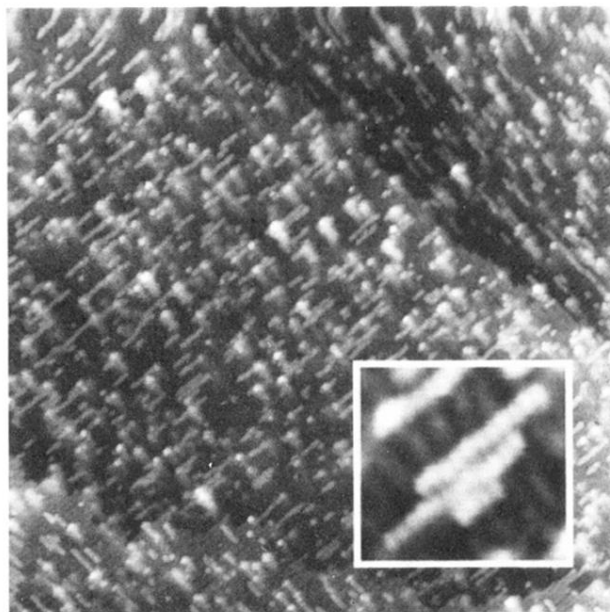


FIG. 4. STM filled state images (+2 V bias) of 50 L of PH_3 adsorption on $\text{Si}(100) 2 \times 1$ at 350°C substrate temperature. The horizontal dimension of the lower-magnification image is ~ 90 nm.

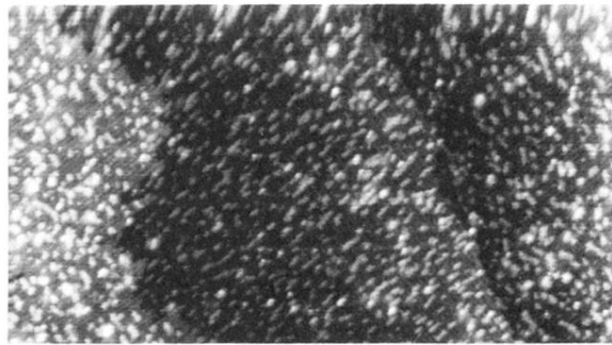


FIG. 5. STM filled state image (+2 V bias) following 0.5 L of PH_3 exposure at RT and annealing the substrate 5 min at 350 °C. The horizontal image size is about 90 nm.

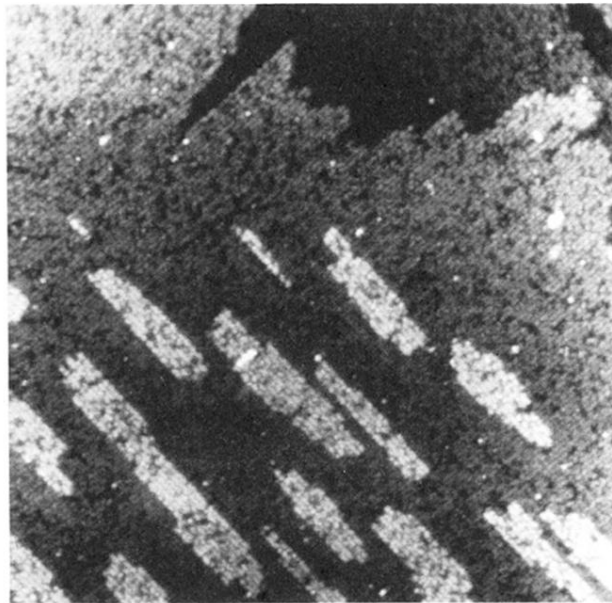


FIG. 6. STM filled state image (+2 V bias) following 5 L of PH_3 exposure at RT and annealing the substrate 5 min at 450°C . The horizontal image size is about 90 nm.

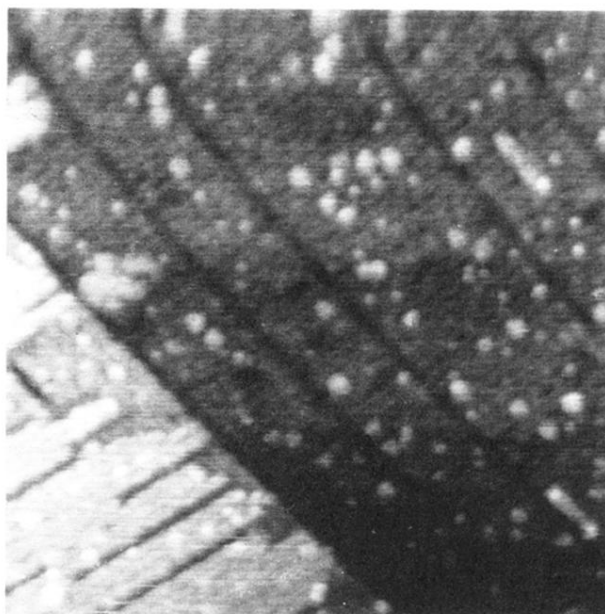


FIG. 7. STM filled state image (+2 V bias) of 50 L of PH_3 adsorption at 625 °C substrate temperature with subsequent 2 min of annealing at 300 °C. The horizontal dimension is ~ 33 nm.

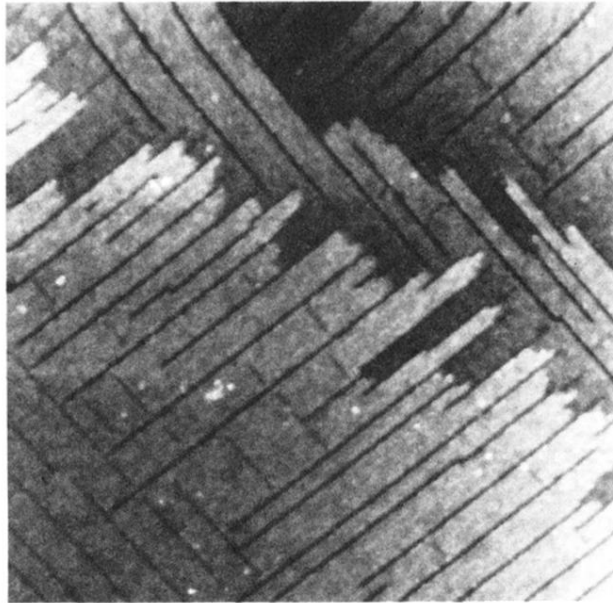


FIG. 8. Large scale ($\sim 90 \times 90 \text{ nm}^2$) STM filled state image (+2 V bias) of the surface shown in Fig. 7 after an additional 5 min of annealing at 500°C . The horizontal dimension is $\sim 90 \text{ nm}$.